CrossMark

A Green and Sustainable Approach for Mild Steel Acidic Corrosion Inhibition Using Leaves Extract: Experimental and DFT Studies

Chandrabhan Verma[1,2] (ID) · M. A. Quraishi[3,4] · Eno E. Ebenso[1,2] · Indra Bahadur[1,2]

Abstract

The effect of *Holoptelea integrifolia* leaf extract (HILE) on corrosive dissolution of mild steel in 1 M hydrochloric acid was investigated using weight loss, surface, electrochemical, and DFT methods. Results showed that corrosion protection capability of HILE increases with increasing its concentration and maximum value of 93.91% was attained at 400 mg/L concentration. Adsorption of phytochemicals present in HILE on metallic surface followed the Langmuir adsorption isotherm. Tafel polarization study revealed that HILE acts as mixed type inhibitor. EIS study revealed that HILE inhibits mild steel corrosion by getting adhered on the mild steel surface. SEM and AFM analyses showed that in presence of HILE, metallic surface becomes smooth because of the formation of inhibitive film over metallic surface. DFT calculations were also performed on the several active phytochemicals. It was found that β-amyrin was the most effective phytochemical for mild steel corrosion among the available constituents present in the extract.

Graphical Abstract
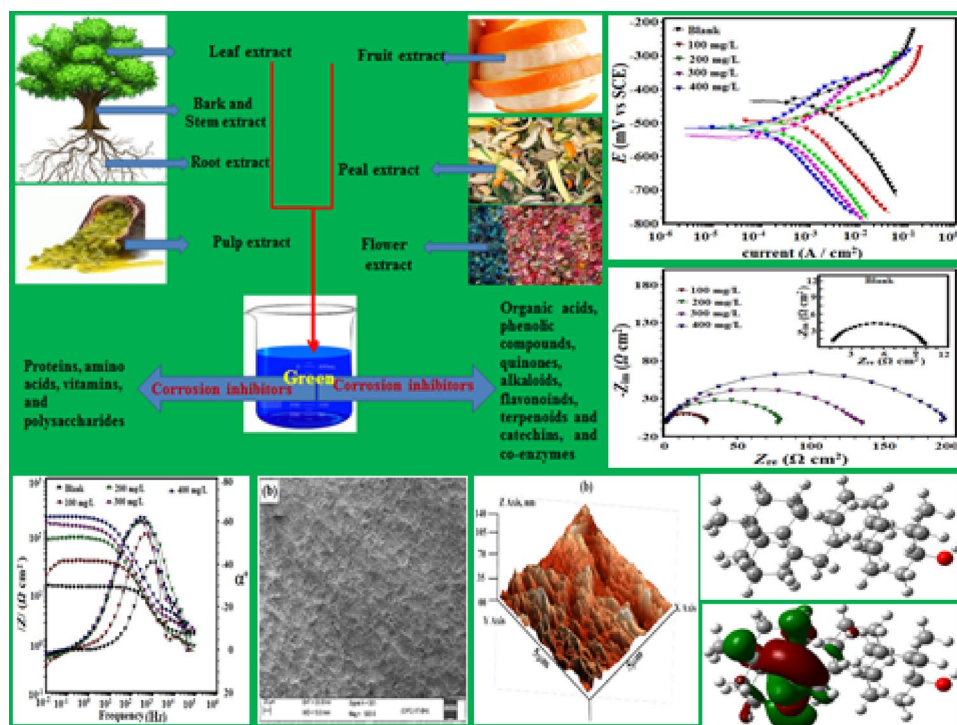
Extended author information available on the last page of the article

1 Introduction

Corrosion is an electrochemical property which deteriorates industrially important metals and alloys into more stable forms such as hydroxides, oxides, and sulfides through direct reactions with the environmental constituents [1, 2]. This is a severe problem to be addressed by industries and educational sectors because it causes enormous economic losses all over the world [3–5]. According to NACE 2016 [3], the economic losses due to corrosion have become about 2.5 trillion US dollars. Among the various available methods, employment of inhibitors is most popular and cost effective approach of corrosion control due to their economic synthesis, facile feasibility, and high efficiency [6–8]. These inhibitors form protective film over metallic surface that separates metal from aggressive corrosive solution, and thereby inhibit corrosion [9]. The high adsorption and inhibition ability of the organic inhibitors is lying on the fact that they can easily transfer as well as accept electrons from the metallic *d*-orbitals and offer strong bonding with them [10–12]. Although, the use of organic inhibitors is one of the most ease, effective and economic methods. However, because of increasing awareness of "green chemistry" in the field of corrosion science and technology throughout the world, there is need to develop some environmental benign corrosion inhibitors [13–15]. "Green chemistry" is a series of principles that reduces the utilization or production of toxic substances in manufacture, design, and application of chemical products [13–15]. Towards the development of "green corrosion inhibitors," several attempts are being made using principals of "green chemistry" such as chemical synthesis involving multicomponent reactions (MCRs), particularly in association with ultrasound and microwave irradiation [14, 16–18], chemical medicines [19], and ionic liquids [20–22].

Most of the organic inhibitors are mostly non-biodegradable and highly toxic for human being as well as for environment [23–25]. The plant extracts derived from different parts of plants such as leaf, stem, root, bark, fruit, peel extract have been extensively used as effective corrosion inhibitors for several metals and alloys in various electrolytic media due to their cost effective, biodegradable, renewable, reliable, versatile, biocompatible, simplicity, and convenient to handle properties [26, 27]. The application of leaf extract as corrosion inhibitor is an environmental friendly, cost effective and green approach for mitigating metallic corrosion, as most of active phytochemicals are water-soluble plant metabolites such as organic acids, phenolic compounds, quinone's, alkaloids, flavonoids, terpenoids and catechins, and co-enzymes, proteins, amino acids, vitamins, and polysaccharides [28].

Generally, the phytochemicals contain several heteroatoms such as nitrogen, oxygen, and sulfur in form of polar fictional groups and heterocyclic rings through which they can adsorb on metal surface and thereby inhibit corrosion [29, 30].

2 Experimental Procedures

2.1 Materials

2.1.1 Preparation of *Holoptelea integrifolia* Leaf Extract

The leaves of *H. integrifolia* were collected from the agricultural field of Varanasi district, Utter Pradesh, India, in the month of September. The methanolic extract of the *H. integrifolia* was prepared as described earlier by Sutar et al. [31]. The *H. integrifolia* leaves powder was charged into the thimble of a Soxhlet apparatus and extracted by methanol. The exhaustive extraction is characterized by appearance of colorless solvent in the siphon tube of Soxhlet apparatus. The methanolic fraction was then heated on water at 50 °C in order to obtain semisolid mass of methanolic extract. This extract was stored in airtight refrigerator below 10 °C.

2.1.2 Electrodes and Reagents

Mild steel specimens having C (0.076%), Si (0.026%), Mn (0.192%), P (0.012%), Al (0.023%), Cr (0.050%), and Fe (balance) were used as test material for electrochemical and surface analytical measurements in test solution of 1 M HCl. The specimens were abraded with emery paper of different grades in order to clean the metallic surface followed by their washing with double deionized water, ultrasonic cleaning in ethanol and finally degreasing with acetone. The cleaned metallic specimens were dried under hot air blower. Test solution 1 M HCl was prepared by the dilution of 37% HCl purchased from MERCK in double distilled water.

2.2 Methods

2.2.1 Experimental Methods

The inhibition tendency of the *H. integrifolia* leaf extract (HILE) was demonstrated using weight loss and electrochemical measurements at 100–400 mg/L concentration, while for the atomic force (AFM) and scanning electron microscopy (SEM) studies 400 mg/L (optimum concentration) was chosen. The weight loss experiment was demonstrated at several concentrations of *H. integrifolia* extract (HILE) ranging from 100 to 400 mg/L. Similarly, instrumentation and methods for surface and electrochemical studies were followed the same as reported previously [32, 33]. Gamry Potentiostat/Galvanostat

with Model G-300 version, Ziess Evo 50 XVP and NT-MDT multimode AFM, Russia containing 111 controlled by solvers scanning probe instruments were used for electrochemical (EIS, Tafel), SEM and AFM analyses, respectively. The preparation of the test specimens and experimental procedure for surface, electrochemical, and weigh loss studies were similar as that have been reported in our earlier studies [32, 33]. Equations (1) to (3) below were employed for evaluation of the inhibition efficiency ($\eta\%$) at the several concentrations of HILE [32, 33]:

$$\eta\% = \frac{w_0 - w_i}{w_0} \times 100 \qquad (1)$$

$$\eta\% = \frac{i_{corr}^0 - i_{corr}^i}{i_{corr}^0} \times 100 \qquad (2)$$

$$\eta\% = \frac{R_{ct}^i - R_{ct}^0}{R_{ct}^i} \times 100 \qquad (3)$$

where w_0 and w_i denote the values of mild steel specimens weight loss after 3-h immersion time without and with leaf extract (HILE), correspondingly. R_{ct}^i and R_{ct}^0 present the charge transfer values for inhibited by *H. integrifolia* leaf extract (HILE) and non-inhibited mild steel specimens, respectively, whereas i_{corr}^i and i_{corr}^0 manifest the current densities values of inhibited and uninhibited metallic specimens, respectively.

2.2.2 DFT Calculations

The *H. integrifolia* leaf extract (HILE) contains several phyto-constituents/phytochemicals that have complex structures with π- and non-bonding electrons by them they can easily adsorb on the metallic surfaces and can protect their corrosion. In the present study, density functional theory (DFT) method has undertaken to describe the adsorption nature of several phytochemicals present in the extract of *H. integrifolia* as described earlier in our research group [34, 35]. The DFT study of some selected phytochemicals was performed using highly sophisticated Gaussian 09 software package. The frontier molecular pictures of the active phytochemicals, namely β-amyrin, friedelin, holoptelin-A, holoptelin-B, 3-epifriedelinol, and stigmasterol, were obtained out at the B3LYP/6-31+G(d,p) level of DFT theory [36]. Based on the values of frontier molecular orbital (FMO) energies (E_{HOMO} and E_{LUMO}), various relative parameters were derived using Eq. (4) to (6) [37, 38]:

$$\Delta E = E_{LUMO} - E_{HOMO} \qquad (4)$$

$$\chi = -\frac{1}{2}\left(E_{LUMO} + E_{HOMO}\right) \qquad (5)$$

$$\Delta N = \frac{\chi_{Fe} - \chi_{inh}}{2\left(\eta_{Fe} + \eta_{inh}\right)} \qquad (6)$$

In the above equations, E_{HOMO} and E_{LUMO} are the energies of FMOs; χ represents the electronegativity; η (it should not be confused with $\eta\%$ used for percentage inhibition efficiency) is the global hardness and ΔN is the fraction of electron transfer. For calculation of values of χ, a value of 0.257 Hartree was employed for electronegativity of the atomic Fe as proposed by the Pearson's electronegativity scale [39], whereas the hardness (η) of bulk Fe was presumed to be equal to 0 Hartree.

3 Results and Discussion

3.1 Gravimetric Measurements

3.1.1 Effect of Extract Concentration

Table 1 represents the protection ability of HILE on mild steel acidic corrosion and various results derived using weight loss experiments after 3-h immersion time 308 K temperature. Inspection of the results showed that the inhibition ability increases with HILE concentration. The highest inhibition efficiency of 94.34% was obtained at 500 mg/L concentration. However, it is also clear from the results that increased concentration from 400 to 500 mg/L did not cause any significant change in the inhibition performance which indicates that 400 mg/L is the optimal concentration. The high inhibition efficiency of HILE is attributed to the presence of several phytochemicals such as terpenoids, steroids, carbohydrates, tannins, proteins, flavones, flavonoids, alkaloids in the methanolic extract of the *H. integrifolia* leaves [34, 35]. In addition to these phytochemicals, *H. integrifolia* extract also contains β-amyrin, friedelin, holoptelin-A, holoptelin-B, 3-epifriedelinol, stigmasterol, etc. [34, 35]. These compounds possess several heteroatoms such as O and N and large carbon skeleton through which they can effectively adsorb over the metallic surface. These adsorbed compounds repelled the aqueous molecules form the surface of the metal

Table 1 The weight loss results obtained for mild steel in 1 M HCl containing different concentrations of *H. integrifolia* leaf extract

Inhibitor	Conc (mg/L)	C_R (mg/cm²/h)	θ	$\eta\%$
Blank	0.0	7.666	–	–
HILE	100	3.933	48.69	0.8969
	200	1.466	80.86	0.8086
	300	0.800	89.56	0.8956
	400	0.466	93.91	0.9391
	500	0.433	94.34	0.9434

and thereby inhibit corrosion. Obviously, increased inhibition efficiency is a consequence of the increase in the surface coverage on enhancing the *H. integrifolia* concentrations.

3.1.2 Effect of Temperature

Weight loss experiment was also carried out at different temperatures (308–338 K) in order to study the influence of temperature on the corrosion inhibition effectiveness of the *H. integrifolia* leaves extract. Results showed that inhibitive property of HILE decreases from 93.91 to 71.78% on increasing solution temperature from 308 to 338 K. This observation is mainly attributed to increased kinetic energy of the phytochemicals/inhibitors present in the extract, at elevated temperature which in turn decreases attraction forces between metal and inhibitor [40, 41]. Moreover, increase in temperature can also cause desorption and molecular rearrangement along with rapid etching and molecular decomposition of the phytochemicals. All these factors adversely affect the inhibition efficiency [40, 41]. The influence of temperature can be best described by Arrhenius equation [42–44]:

$$\log(C_{\mathrm{R}}) = \frac{-E_{\mathrm{a}}}{2.303RT} + \log A \qquad (7)$$

In the Arrhenius equation, C_{R} denotes the corrosion rate (mg/cm^2/h); R represents the universal gas constant, and T presents the absolute temperature. A is the Arrhenius preexponential factor, and E_{a} is the activation energy for corrosion process. Arrhenius plots for mild steel dissolution in 1 M HCl are shown in Fig. 1, which represents straight lines between log C_{R} and 1/T. The values of activation energies for both metallic specimens were derived from the slope
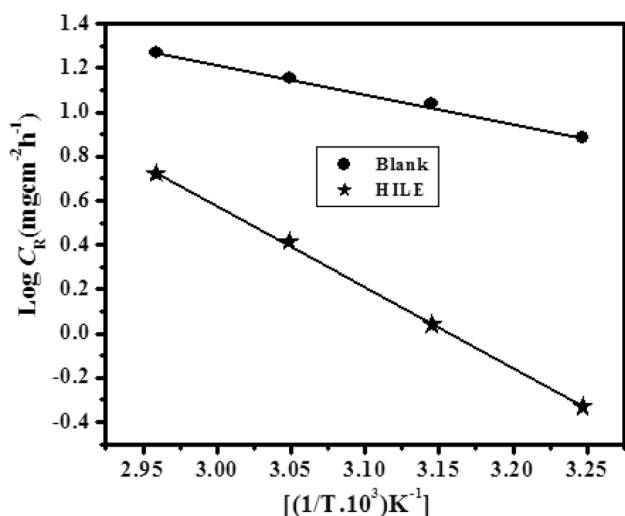
$(-\Delta E_{\mathrm{a}}/2.303R)$ of Arrhenius plots. The values of E_{a} were 28.48 and 70.44 kJ/mol for uninhibited and inhibited specimens, respectively. Increased value of E_{a} for inhibited specimen indicates that metallic dissolution has become difficult owing to formation of energy barrier for corrosion taking place [45, 46].

3.2 Adsorption Isotherm

In order to describe the adsorption behavior of HILE on mild steel surface, several isotherms including Temkin, Frumkin, Freundlich, and Langmuir isotherms were tested among which Langmuir adsorption isotherm showed the best fit. The values of regression coefficients (R^2) were used as selection criterion for the best isotherm. It is important to mention that the value of R^2 was most close to unity for Langmuir isotherm ($R^2 = 0.9982$; Fig. 2); however, value of slope was much deviated from ideal Langmuir adsorption isotherm behavior as its value is much apart from one. This deviation from ideal Langmuir behavior is attributed to intermolecular interactions between adsorbed inhibitor molecules and change in the metallic surface energy that are not considered during the formulation of Langmuir isotherm formula [46]. In best way, the Langmuir isotherm is represented as follows:

$$K_{\mathrm{ads}}C = \frac{\theta}{1-\theta} \qquad (8)$$

In the Langmuir isotherm, K_{ads} is the Langmuir constant, commonly called as adsorption–desorption constant; C is the concentration of inhibitor, and θ is the surface coverage. The K_{ads} values for HILE at different temperature were calculated from the intercept of Langmuir

Fig. 1 Arrhenius plots for the corrosion of mild steel in 1 M HCl without and with the inhibitor
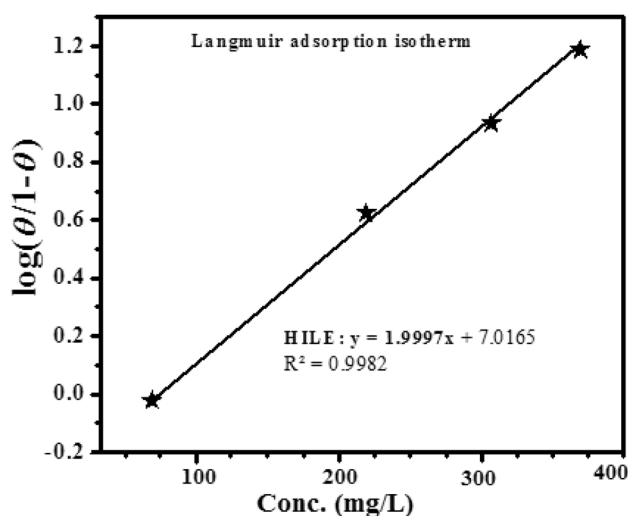

Fig. 2 Langmuir adsorption isotherm plots for the adsorption of HILE on mild steel surface in 1 M HCl

Table 2 Values of $-\Delta G^0_{ads}$ and K_{ads} for mild steel in 1 M HCl at different temperatures

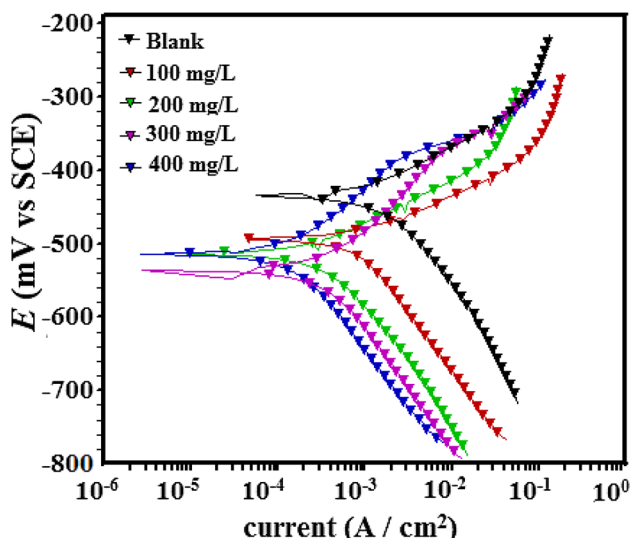| Inhibitor	K_{ads} (10^4 M^{-1})				$-\Delta G^0_{ads}$ (kJ/mol)			
Temperature (K)	308	318	328	338	308	318	328	338
HILE	1.85	1.08	0.54	0.30	35.45	35.18	34.40	33.84

Fig. 3 Potentiodynamic polarization curves for mild steel corrosion in 1 M HCl in the absence and presence of different concentrations of the HILE

adsorption isotherm, through which values of standard Gibb's free energy (ΔG^0_{ads}) were derived using the following equation [46]:

$$\Delta G^0_{ads} = -RT \ln \left(55.5 K_{ads} \right) \qquad (9)$$

In above equation, numerical value 55.5 denotes the aqueous (water) concentration in acid solution (1 M HCl). The calculated value of K_{ads} and ΔG^0_{ads} is shown in Table 2. Generally, a high value of K_{ads} manifests strong interaction between inhibitor and the surface of metals. In our present study, values of K_{ads} are of 10^4 orders which indicate that HILE has strong propensity of adsorption over the metallic surfaces. Results showed that values of ΔG^0_{ads} range between −35.45 and −33.84 kJ/mol, indicating that adsorption of HILE on the metallic surface involves mixed mode of adsorption [47].

3.3 Electrochemical Studies

3.3.1 Tafel Polarization

The Tafel polarization curves for inhibited and uninhibited mild steel specimens are shown in Fig. 3, and several electrochemical polarization parameters including anodic and cathodic Tafel slopes (β_a, and β_c), corrosion potential (E_{corr}), corrosion current density (i_{corr}), and corresponding percentage inhibition efficiency are given in Table 3. Inspection of the results showed that in the presence of HILE, values of corrosion current decreased significantly without changing the shape of polarization curves which suggests that HILE inhibits corrosion by blocking the active sites present on the metallic surface without changing the mechanism of corrosion [48]. The results further showed that maximum displacement in the E_{corr} value for inhibited specimen with respect to uninhibited specimen was 68 mV, which indicates that HILE acts as mixed type inhibitor. The values of cathodic slopes (β_c) much deviated as compared to the values of anodic slope (β_a), which suggested that investigated leaves extract behaves as mixed type but predominantly cathodic-type inhibitor.

3.3.2 Electrochemical Impedance Spectroscopy (EIS) Study

The fitted Nyquist curves in the absence and presence of HILE are presented in Fig. 4. Figure 5 represents the Nyquist plots for corrosion of testing specimens in 1 M hydrochloric acid solution examination of which shows that diameter of the Nyquist plots is much higher in the presence of inhibitor than in their absence. Moreover, the diameter of the Nyquist plots increases with increasing inhibitor concentration. Generally, during interpretation of Nyquist plots difference between the real impedances at high and low lower frequencies is regarded as charge transfer resistance (R_{ct}). However, it is obvious that metal corroding acid solution particularly in the presence of

Table 3 Tafel polarization parameters for mild steel in 1 M HCl solution in absence and at different concentrations of *H. integrifolia* leaf extract

Inhibitor	Conc (mg/L)	E_{corr} (mV/SCE)	β_a (µA/cm²)	β_c (mV/dec)	i_{corr} (mV/dec)	$\eta\%$	θ
Blank	–	−445	70.5	114.6	1150	–	–
HILE	100	−504	56.20	198.1	936.0	18.60	0.18.60
	200	−513	78.90	210.2	218.0	81.04	0.8104
	300	−511	70.60	91.60	132.0	88.52	0.8852
	400	−510	79.90	123.8	117.0	89.82	0.8982

Fig. 4 Fitted Nyquist plots of impedance spectra of mild steel in 1 M HCl in the absence and presence of HILE
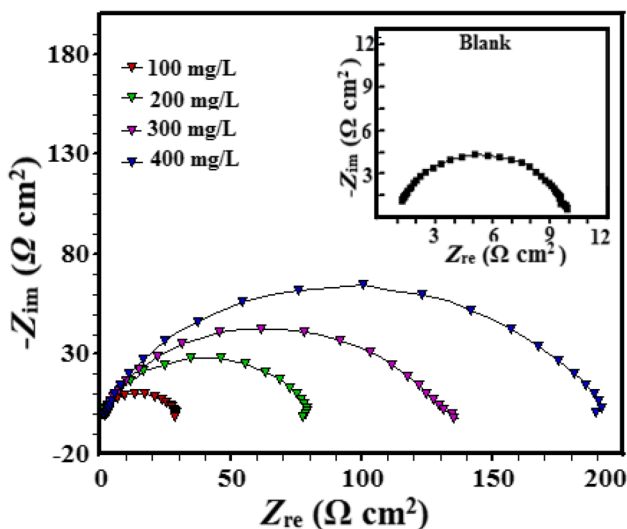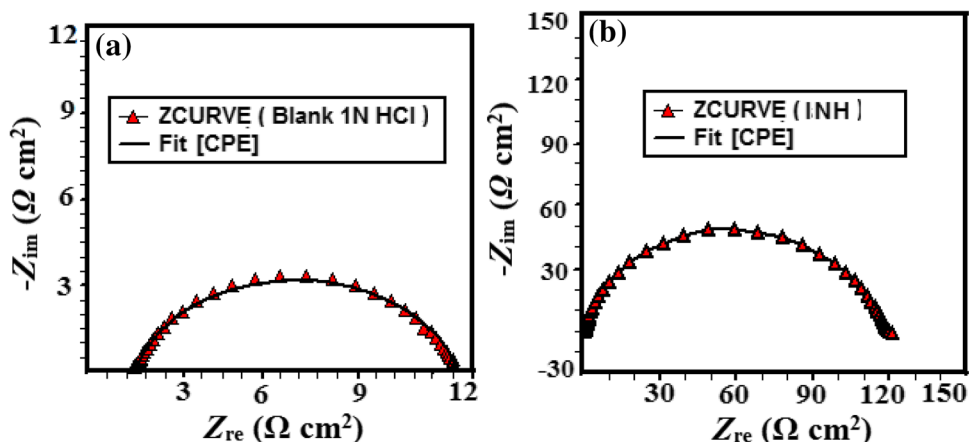

Fig. 5 Nyquist plot for mild steel in 1 M HCl in the absence and presence of different concentrations of HILE

inhibitor is associated with several other kinds of resistances such as resistance due to accumulation of corrosion products i.e., accumulation resistance (R_a), resistance due to inhibitor film i.e., film resistance, (R_f), and diffusion layer resistance (R_d). Therefore, in present case, polarization resistance ($R_p = R_a + R_f + R_d$) was undertaken rather than charge transfer resistance (R_{ct}). All electrochemical data were examined by employing a suitable equivalent circuit described earlier [49–51]. For metal dissolution

under acidic environments, better approximation has been observed when capacitance is replaced by constant phase element (CPE). The impedance of the constant phase element (CPE) can be represented as follows:

$$Z_{CPE} = \left(\frac{1}{Y_0}\right)\left[(j\omega)^n\right]^{-1} \tag{10}$$

In above equation, Y_0 is the CPE constant'; j represents the imaginary number; ω denotes the angular frequency, and n is the phase shift which measures of surface homogeneity. In general, a higher value of phase shift suggests high surface smoothness. In addition to the surface roughness, phase shift also gives information about the nature of CPE as $n = 0$ represents resistor, $n = 1$ represents capacitance, $n = -1$ represents inductance and $n = 0.5$ signifies Warburg impedance. EIS results depicted in Table 4 revealed that values of n in present case vary in between 0.757 and 0.827 indicating that CPE behaves as capacitances. Deviation from perfect capacitive performance (deviation from $n = 1$) is attributed to surface inhomogeneity. The double layer capacitance (C_{dl}) was derived through the following relationship:

$$C_{dl} = Y_0(\omega_{max})^{n-1} \tag{11}$$

where ω_{max} represents that frequency at which the imaginary part of impedance has acquired the maximum (rad/s) value. From the results (Table 4), it is observed that values of R_p increase while values of C_{dl} decrease on increasing the

Table 4 EIS parameters obtained for mild steel in 1 M HCl in the absence and presence of different concentrations of *H. integrifolia* leaf extract

Inhibitor	Conc (mg/L)	R_s (Ω cm^2)	R_p (Ω cm^2)	n	C_{dl} (μF/cm)	L (Ω cm^2)	$\eta\%$	θ
Blank	–	1.12	9.58	0.827	106.21	–	–	–
HILE	100	0.828	24.382	0.826	91.25	4	49.79	0.4979
	200	0.779	76.421	0.785	105.89	7	83.98	0.8398
	300	0.932	125.268	0.757	60.18	–	90.23	0.9023
	400	2.022	184.178	0.802	60.48	6	93.35	0.9335

concentration of inhibitor. This observation indicates that studied inhibitor inhibits metallic corrosion by adsorbing on the metal (mild steel)/electrolyte (1 M HCl) interfaces [52].

The adsorption behavior of HILE on the metal/electrolyte interfaces was further investigated by Bode plots (Fig. 6), plotted for inhibited and uninhibited mild steel specimens. As stated earlier, a perfect capacitor is defined by the values of slopes and phase angles $(\alpha^0) - 1°$ and $-90°$, respectively. However, in present case, Bode plots between log |Z| versus log f represent values of slopes and phase angle nearly $-0.84°$ and $-70°$, respectively. This type deviation again
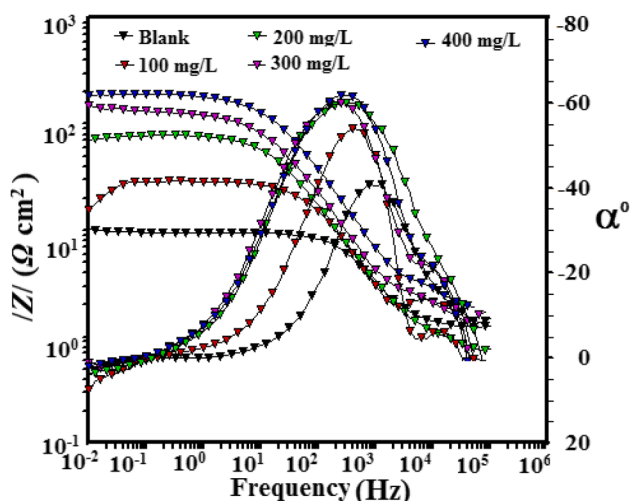
attributed to surface inhomogeneity resulted due to structural and interfacial origin [53, 54]. However, in the presence of HILE (Fig. 6), values of phase angle have enhanced indicating significant improvement in the surface smoothness due to development of protective film by inhibitor over metallic surface which separates metal (mild steel) surfaces from aggressive acid solution and thereby protects from corrosion [53, 54].

3.4 Surface Analyses

3.4.1 SEM Study

SEM micrographs of inhibited and uninhibited mild steel specimens after 3-h corrosion in 1 M HCl are shown in Fig. 7. The metallic surface was highly damaged and corroded for uninhibited mild steel specimen (Fig. 7a), which could be as a consequence of free acid attack of metallic surface in the absence of inhibitor. However, in the presence of optimum concentration of HILE (Fig. 7b), the metallic surface became significantly smooth. This finding suggests that HILE inhibits the corrosion of mild steel because of its presence in the aggressive acid solution.

3.4.2 AFM Study

The surface morphologies of mild steel specimens under consideration were also investigated using AFM method in order to support the results of other experimental methods. AFM micrographs of mild steel corroded for 3-h immersion time in 1 M HCl with and without inhibitors are shown in
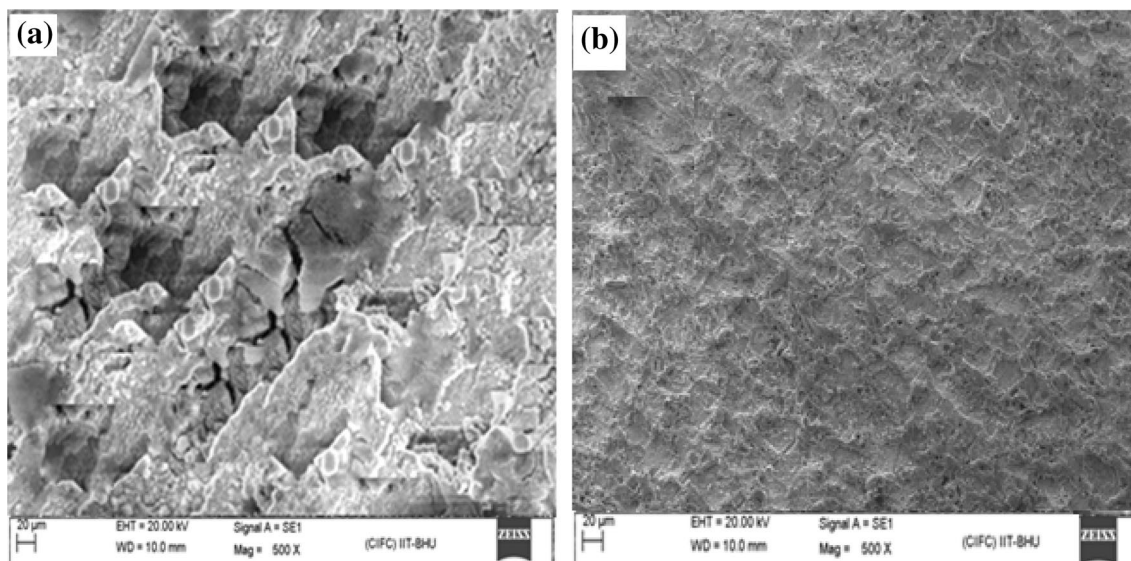

Fig. 6 Bode plots for mild steel in 1 M HCl in the absence and presence of different concentrations of HILE

Fig. 7 Scanning electron microscope (SEM) micrographs of mild steel surface after 3-h immersion time in 1 M hydrochloric acid solution; without (**a**) and with (**b**) optimum concentration of HILE
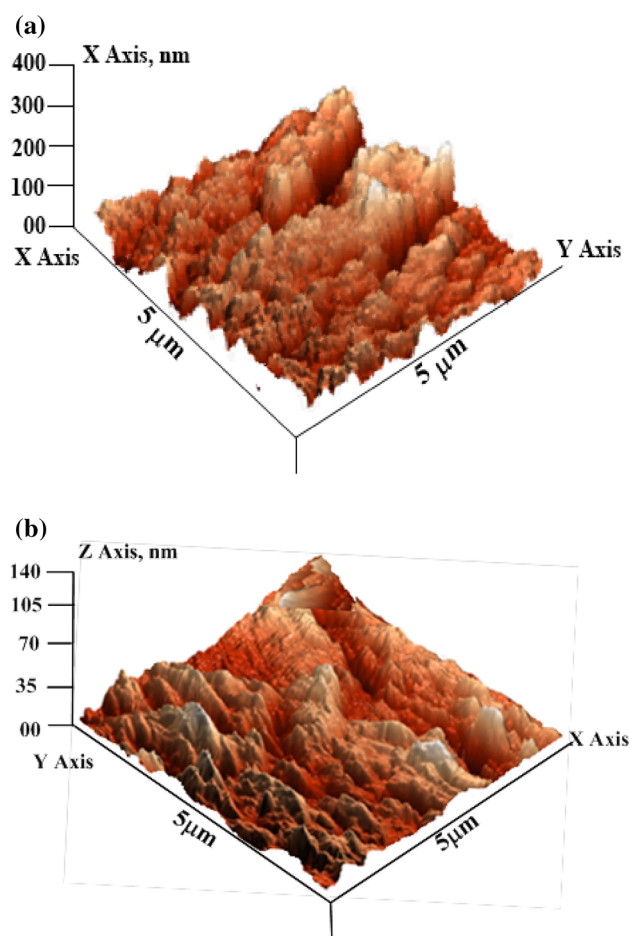
(a)

(b)

Fig. 8 Atomic force microscope (AFM) micrographs of mild steel surface after 3-h immersion time in 1 M hydrochloric acid solution; without (**a**) and with (**b**) optimum concentration of HILE

Fig. 8. Inspection of Fig. 8 showed that metal surface was highly corroded resulted in very high surface roughness. Very high corrosion rate by aggressive acidic attack makes the surface very rough that have average surface roughness of 392 nm. AFM micrographs inhibited by HILE at its 400 mg/L concentration are relatively smoother and less damaged owing to the adsorption of phytochemicals over the metallic surface. The estimated surface roughness (average) was 124 nm in the presence of HILE.

3.5 Quantum Chemical Calculations

The frontier molecular electron distribution of the active phytochemicals namely, β-amyrin, friedelin, holoptelin-A, holoptelin-B, 3-epifriedelinol, and stigmasterol of the *H. integrifolia* leaf extract is shown in Fig. 9 and several quantum chemical calculation indices are presented in Table 5. Generally, E_{HOMO} represents the electron donating tendency of a chemical species to the accepting molecule, while E_{LUMO} represents the electron accepting property of

the molecule from donor molecule [53, 54]. From the parameters represented in Table 5, it is seen that friedelin has highest, while 3-epifriedelinol has lowest value of E_{HOMO}, indicating that friedelin has strongest tendency, whereas 3-epifriedelinol has lowest electron donating ability among the investigated active components. The values of E_{LUMO} did not give any regular trends in the present study. The energy band gap, ΔE ($E_{LUMO} - E_{HOMO}$), is an important and commonly used reactivity parameter, which describes the relative affinities of several components of *H. integrifolia* leaf extract towards metallic surface. In general, lower value of ΔE is allied with high chemical reactivity and thereby high inhibition performance. In present case, β-amyrin is associated with lowest value of ΔE, while 3-epifriedelinol is associated with highest value of ΔE. This finding suggests that β-amyrin has maximum and 3-epifriedelinol has lowest chemical reactivity. Values of global hardness (η) and softness (σ) were also derived and given in Table 5. A low value of hardness and high value softness associated with high chemical reactivity and therefore higher inhibition efficiency. Among the investigated components, β-amyrin is associated with lowest value of hardness and highest value of softness suggesting that it is the most active component of the *H. integrifolia* leaf extract, while converse is also true for 3-epifriedelinol. Values of absolute electronegativity (χ) did not show any regular trends. However, fraction of electron transfer (ΔN) is maximum for β-amyrin and lowest for 3-epifriedelinol suggesting that latter has highest electron donating ability to the metallic surface, while former has lowest. Dipole moment (μ) is another important parameter which can be used to describe relative affinity of the studied phytochemicals towards metallic surface. Molecules having high value of dipole moment are associated with their high polarizability therefore high surface area. Therefore, it can be concluded that the component which has maximum dipole moment is most effective component. From results depicted in Table 5, it can be seen that β-amyrin is the most active component among the investigated phytochemicals as it is associated with maximum value of dipole moment.

4 Conclusions

The inhibition effect of *H. integrifolia* leaf extract has been investigated in the present investigation using experimental and DFT approaches. Results of the present study led to derivation of following conclusions:

1. *H. integrifolia* leaf extract acts as green and efficient inhibitor for mild steel corrosion in 1 M hydrochloric acid and its inhibition performance increases with increasing its concentration. It showed highest efficiency of 94.34% at 400 mg/L concentration.
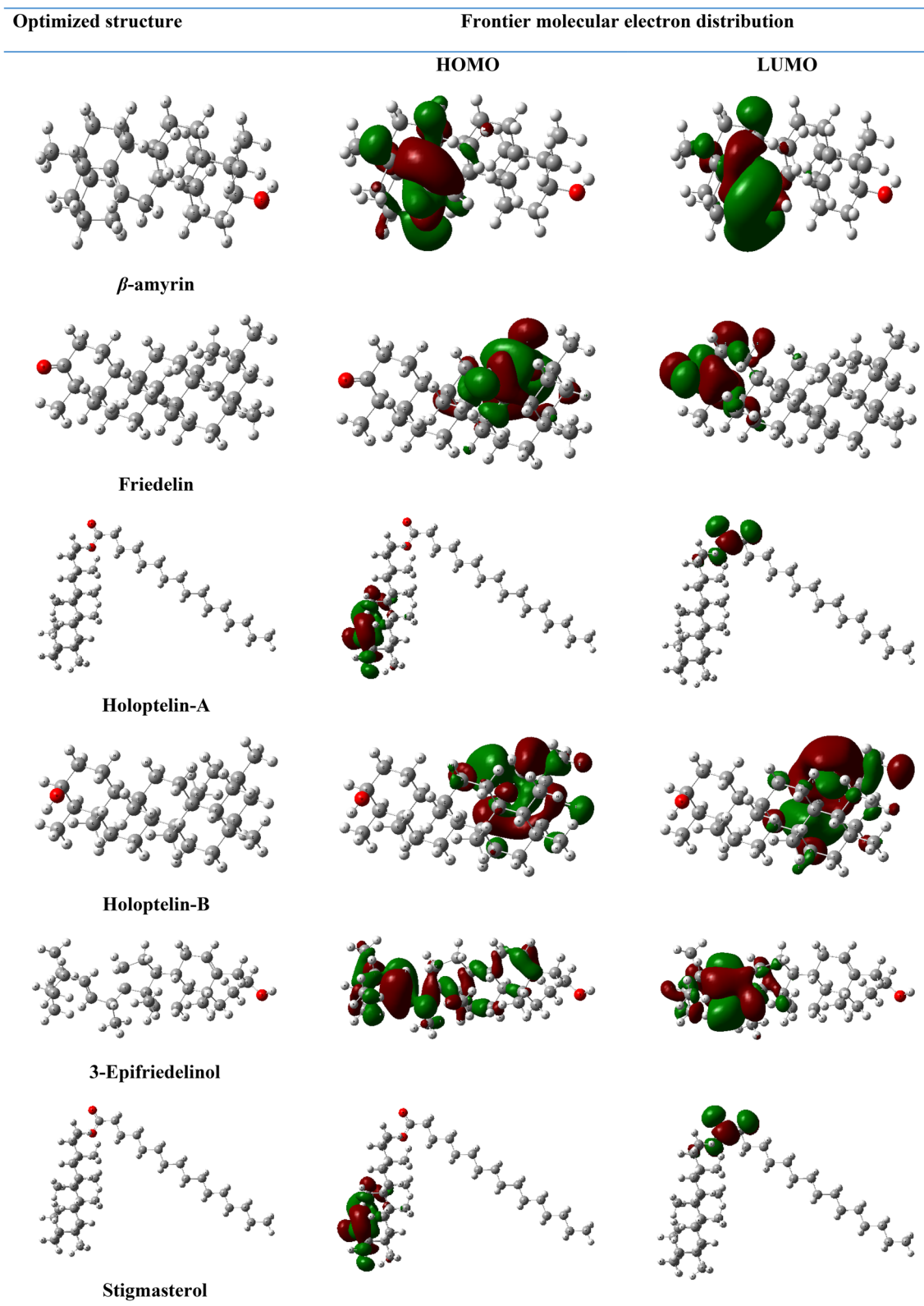
Optimized structure	Frontier molecular electron distribution	
	HOMO	LUMO

β-amyrin

Friedelin

Holoptelin-A

Holoptelin-B

3-Epifriedelinol

Stigmasterol

Fig. 9 Optimized molecular structures, highest occupied and lowest unoccupied frontier molecular orbital pictures of active phytochemicals present in leaves extract of *H. integrifolia*

Table 5 Quantum chemical calculation parameters for different active constituents of the *H. integrifolia* leaf extract

Constituents	Parameters							
	E_{HOMO} (Hartree)	E_{LUMO} (Hartree)	ΔE (Hartree)	χ	η	σ	ΔN	μ (Debye)
β-Amyrin	−0.149	−0.012	0.136	0.081	0.068	14.608	1.286	0.788
Friedelin	−0.037	−0.010	0.027	0.024	0.013	73.773	8.589	4.106
Holoptelin-A	−0.038	0.003	0.041	0.017	0.020	47.881	5.736	2.027
Holoptelin-B	−0.039	0.020	0.059	0.009	0.029	33.818	4.188	1.418
3-Epifriedelinol	−0.215	0.015	0.230	0.100	0.115	8.689	0.682	1.468
Stigmasterol	−0.038	0.003	0.041	0.017	0.020	47.846	5.732	2.028

2. Adsorption of *H. integrifolia* leaf extract on metallic surface obeyed the Langmuir adsorption isotherm.
3. Tafel polarization study revealed that HILE acts as mixed inhibitor and predominantly shows cathodic behavior.
4. EIS study suggests that HILE inhibits corrosion by adsorbing on the metal/electrolyte interfaces.
5. Adsorption of HILE on metal surface was further supported by SEM and AFM analysis where significant surface smoothness was obtained in the presence of inhibitor.
6. DFT study provides good insight about inhibition performance of several active phytochemicals present in the *H. integrifolia* leaf extract. The quantum chemical calculation results showed that *β*-amyrin is the most active phytochemical present in the leaves extract.

References

1. Mai W, Soghrati S, Buchheit RG (2016) A phase field model for simulating the pitting corrosion. Corros Sci 110:157–166
2. Kıcır N, Tansuğ G, Erbil M, Tüken T (2016) Investigation of ammonium (2, 4-dimethylphenyl)-dithiocarbamate as a new, effective corrosion inhibitor for mild steel. Corros Sci 105:88–99
3. Gupta RK, Malviya M, Verma C, Quraishi M (2017) Aminoazobenzene and diaminoazobenzene functionalized graphene oxides as novel class of corrosion inhibitors for mild steel: experimental and DFT studies. Mater Chem Phys 198:360–373
4. Alibakhshi E, Ramezanzadeh M, Bahlakeh G, Ramezanzadeh B, Mahdavian M, Motamedi M (2018) Glycyrrhiza glabra leaves extract as a green corrosion inhibitor for mild steel in 1 M hydrochloric acid solution: experimental, molecular dynamics, Monte Carlo and quantum mechanics study. J Mol Liq 255:185–198
5. Zhang F, Tang Y, Cao Z, Jing W, Wu Z, Chen Y (2012) Performance and theoretical study on corrosion inhibition of 2-(4-pyridyl)-benzimidazole for mild steel in hydrochloric acid. Corros Sci 61:1–9
6. Ehsani A, Mahjani M, Hosseini M, Safari R, Moshrefi R, Shiri HM (2017) Evaluation of *Thymus vulgaris* plant extract as an eco-friendly corrosion inhibitor for stainless steel 304 in acidic solution by means of electrochemical impedance spectroscopy, electrochemical noise analysis and density functional theory. J Colloid Interface Sci 490:444–451
7. Liu F, Zhang L, Yan X, Lu X, Gao Y, Zhao C (2015) Effect of diesel on corrosion inhibitors and application of bio-enzyme corrosion inhibitors in the laboratory cooling water system. Corros Sci 93:293–300
8. Sin HLY, Rahim AA, Gan CY, Saad B, Salleh MI, Umeda M (2017) *Aquilaria subintergra* leaves extracts as sustainable mild steel corrosion inhibitors in HCl. Measurement 109:334–345
9. Ramezanzadeh M, Sanaei Z, Bahlakeh G, Ramezanzadeh B (2018) Highly effective inhibition of mild steel corrosion in 3.5% NaCl solution by green Nettle leaves extract and synergistic effect of eco-friendly cerium nitrate additive: experimental, MD simulation and QM investigations. J Mol Liq 256:67–83
10. Li X, Xie X, Deng S, Du G (2014) Two phenylpyrimidine derivatives as new corrosion inhibitors for cold rolled steel in hydrochloric acid solution. Corros Sci 87:27–39
11. Guo L, Zhu S, Zhang S, He Q, Li W (2014) Theoretical studies of three triazole derivatives as corrosion inhibitors for mild steel in acidic medium. Corros Sci 87:366–375
12. Umoren SA, Eduok UM (2016) Application of carbohydrate polymers as corrosion inhibitors for metal substrates in different media: a review. Carbohydr Polym 140:314–341
13. Mohammadinejad R, Karimi S, Iravani S, Varma RS (2016) Plant-derived nanostructures: types and applications. Green Chem 18:20–52
14. Varma RS (2014) Journey on greener pathways: from the use of alternate energy inputs and benign reaction media to sustainable applications of nano-catalysts in synthesis and environmental remediation. Green Chem 16:2027–2041
15. Jeon H, Lim C, Lee JM, Kim S (2015) Chemical assay-guided natural product isolation via solid-supported chemodosimetric fluorescent probe. Chem Sci 6:2806–2811
16. Namboodiri VV, Varma RS (2002) Solvent-free sonochemical preparation of ionic liquids. Org Lett 4:3161–3163
17. Singh MS, Chowdhury S (2012) Recent developments in solvent-free multicomponent reactions: a perfect synergy for eco-compatible organic synthesis. RSC Adv 2:4547–4592
18. Cioc RC, Ruijter E, Orru RV (2014) Multicomponent reactions: advanced tools for sustainable organic synthesis. Green Chem 16:2958–2975
19. Gece G, Drugs (2011) A review of promising novel corrosion inhibitors. Corros Sci 53:3873–3898
20. Yesudass S, Olasunkanmi LO, Bahadur I, Kabanda MM, Obot I, Ebenso EE (2016) Experimental and theoretical studies on some selected ionic liquids with different cations/anions as corrosion inhibitors for mild steel in acidic medium. J Taiwan Inst Chem Eng 64:252–268

21. Diamanti MV, Velardi UV, Brenna A, Mele A, Pedeferri M, Ormellese M (2016) Compatibility of imidazolium-based ionic liquids for CO_2 capture with steel alloys: a corrosion perspective. Electrochim Acta 192:414–421

22. Lozano I, Mazario E, Olivares-Xometl C, Likhanova N, Herrasti P (2014) Corrosion behaviour of API 5LX52 steel in HCl and H_2SO_4 media in the presence of 1, 3-dibencilimidazolio acetate and 1, 3-dibencilimidazolio dodecanoate ionic liquids as inhibitors. Mater Chem Phys 147:191–197

23. Muthukrishnan P, Jeyaprabha B, Prakash P (2017) Adsorption and corrosion inhibiting behavior of *Lannea coromandelica* leaf extract on mild steel corrosion. Arab J Chem 10:S2343–S2354

24. Hassan KH, Khadom AA, Kurshed NH (2016) *Citrus aurantium* leaves extracts as a sustainable corrosion inhibitor of mild steel in sulfuric acid. S Afr J Chem Eng 22:1–5

25. Gerengi H, Uygur I, Solomon M, Yildiz M, Goksu H (2016) Evaluation of the inhibitive effect of *Diospyros kaki* (Persimmon) leaves extract on St37 steel corrosion in acid medium. Sustain Chem Pharm 4:57–66

26. Loto RT, Loto CA, Joseph O, Olanrewaju G (2016) Adsorption and corrosion inhibition properties of thiocarbanilide on the electrochemical behavior of high carbon steel in dilute acid solutions. Results Phys 6:305–314

27. Dehdab M, Yavari Z, Darijani M, Bargahi A (2016) The inhibition of carbon-steel corrosion in seawater by streptomycin and tetracycline antibiotics: an experimental and theoretical study. Desalination 400:7–17

28. Madkour LH, Kaya S, Kaya C, Guo L (2016) Quantum chemical calculations, molecular dynamics simulation and experimental studies of using some azo dyes as corrosion inhibitors for iron. Part 1: mono-azo dye derivatives. J Taiwan Inst Chem Eng 68:461–480

29. Tezeghdenti M, Dhouibi L, Etteyeb N (2015) Corrosion inhibition of carbon steel in 1 M sulphuric acid solution by extract of *Eucalyptus globulus* leaves cultivated in Tunisia Arid zones. J Bio Tribo-Corros 1:16

30. Khadraoui A, Khelifa A, Hamitouche H, Mehdaoui R (2014) Inhibitive effect by extract of *Mentha rotundifolia* leaves on the corrosion of steel in 1 M HCl solution. Res Chem Intermed 40:961–972

31. Sutar RC, Kasture SB, Kalaichelvan V (2014) Evaluation of antidepressant activity of leaf extracts of *Holoptelea integri* Folia (roxb) planch in experimental animals. Int J Pharm Pharm Sci 6:250–253

32. Reddy MJ, Verma CB, Ebenso E, Singh K, Quaraishi M (2014) Electrochemical and thermodynamic investigation of nitrofurantoin as effective corrosion inhibitor for mild steel in 1M hydrochloric acid solution. Int J Electrochem Sci 9:4884–4899

33. Verma C, Quraishi M, Kluza K, Makowska-Janusik M, Olasunkanmi LO, Ebenso EE (2017) Corrosion inhibition of mild steel in 1M HCl by D-glucose derivatives of dihydropyrido [2, 3-d: 6, 5-d′] dipyrimidine-2, 4, 6, 8 (1H, 3H, 5H, 7H)-tetraone. Sci Rep 7:44432

34. Kumar D, Kumar K, Gupta J, Bishnoi N, Kumar S (2012) A mini review on chemistry and biology of *Holoptelea integrifolia* Roxb. Planch (Ulmaceae). Asian Pac J Trop Biomed 2:S1200–S1205

35. Aadesh U (2010) Anti-inflammatory evaluation of ethanolic extract of leaves of *Holoptelea integrifolia*, Planch. Ann Biol Res 1:185–195

36. Martinez S (2003) Inhibitory mechanism of mimosa tannin using molecular modeling and substitutional adsorption isotherms. Mater Chem Phys 77:97–102

37. Yadav M, Kumar S, Purkait T, Olasunkanmi L, Bahadur I, Ebenso E (2016) Electrochemical, thermodynamic and quantum chemical studies of synthesized benzimidazole derivatives as corrosion inhibitors for N80 steel in hydrochloric acid. J Mol Liq 213:122–138

38. Olasunkanmi LO, Kabanda MM, Ebenso EE (2016) Quinoxaline derivatives as corrosion inhibitors for mild steel in hydrochloric acid medium: electrochemical and quantum chemical studies. Physica E 76:109–126

39. Pearson RG (1988) Absolute electronegativity and hardness: application to inorganic chemistry. Inorg Chem 27:734–740

40. Verma C, Quraishi M, Singh A (2015) 2-Amino-5-nitro-4, 6-diarylcyclohex-1-ene-1, 3, 3-tricarbonitriles as new and effective corrosion inhibitors for mild steel in 1 M HCl: experimental and theoretical studies. J Mol Liq 212:804–812

41. Verma C, Quraishi M, Singh A (2016) 5-Substituted 1H-tetrazoles as effective corrosion inhibitors for mild steel in 1 M hydrochloric acid. J Taibah Univ Sci 10:718–733

42. Saxena A, Prasad D, Haldhar R, Singh G, Kumar A (2018) Use of *Saraca ashoka* extract as green corrosion inhibitor for mild steel in 0.5 M H_2SO_4. J Mol Liq 258:89–97

43. Al-Moubaraki AH, Al-Howiti AA, Al-Dailami MM, Al-Ghamdi EA (2017) Role of aqueous extract of celery (*Apium graveolens* L.) seeds against the corrosion of aluminium/sodium hydroxide systems. J Environ Chem Eng 5:4194–4205

44. Khadom AA, Abd AN, Ahmed NA (2018) *Xanthium strumarium* leaves extracts as a friendly corrosion inhibitor of low carbon steel in hydrochloric acid: kinetics and mathematical studies. S Afr J Chem Eng 25:13–21

45. Liao LL, Mo S, Luo HQ, Li NB (2017) Longan seed and peel as environmentally friendly corrosion inhibitor for mild steel in acid solution: experimental and theoretical studies. J Colloid Interface Sci 499:110–119

46. Alvarez PE, Fiori-Bimbi MV, Neske A, Brandán SA, Gervasi CA (2018) *Rollinia occidentalis* extract as green corrosion inhibitor for carbon steel in HCl solution. J Ind Eng Chem 58:92–99

47. Gupta NK, Quraishi M, Verma C, Mukherjee A (2016) Green Schiff's bases as corrosion inhibitors for mild steel in 1 M HCl solution: experimental and theoretical approach. RSC Adv 6:102076–102087

48. Chauhan L, Gunasekaran G (2007) Corrosion inhibition of mild steel by plant extract in dilute HCl medium. Corros Sci 49:1143–1161

49. Verma C, Quraishi M, Ebenso E, Obot I, El A, Assyry A (2016) 3-Amino alkylated indoles as corrosion inhibitors for mild steel in 1M HCl: experimental and theoretical studies. J Mol Liq 219:647–660

50. Solmaz R, Kardaş G, Culha M, Erbil M (2008) Investigation of adsorption and inhibitive effect of 2-mercaptothiazoline on corrosion of mild steel in hydrochloric acid media. Electrochim Acta 53:5941–5952

51. Solmaz R, Kardaş G, Erbil M (2008) Adsorption and corrosion inhibitive properties of 2-amino-5-mercapto-1, 3, 4-thiadiazole on mild steel in hydrochloric acid media. Colloids Surf A 312:7–17

52. Lebrini M, Robert F, Lecante A, Roos C (2011) Corrosion inhibition of C38 steel in 1 M hydrochloric acid medium by alkaloids extract from *Oxandra asbeckii* plant. Corros Sci 53:687–695

53. Verma C, Quraishi M, Singh A (2016) A thermodynamical, electrochemical, theoretical and surface investigation of diheteroaryl thioethers as effective corrosion inhibitors for mild steel in 1 M HCl. J Taiwan Inst Chem Eng 58:127–140

54. Verma C, Olasunkanmi LO, Ebenso EE, Quraishi MA, Obot IB (2016) Adsorption behavior of glucosamine-based, pyrimidine-fused heterocycles as green corrosion inhibitors for mild steel: experimental and theoretical studies. J Phys Chem C 120:11598–11611

Affiliations

Chandrabhan Verma[1,2] (iD) **· M. A. Quraishi[3,4] · Eno E. Ebenso[1,2] · Indra Bahadur[1,2]**

✉   Chandrabhan Verma
   chandraverma.rs.apc@itbhu.ac.in; cbverma38@gmail.com

[1]   Department of Chemistry, Faculty of Agriculture, Science
   and Technology, North-West University (Mafikeng Campus),
   Private Bag X2046, Mmabatho 2735, South Africa

[2]   Material Science Innovation & Modelling (MaSIM) Research
   Focus Area, Faculty of Agriculture, Science and Technology,
   North-West University (Mafikeng Campus), Private Bag
   X2046, Mmabatho 2735, South Africa

[3]   Center of Research Excellence in Corrosion, Research
   Institute, King Fahd University of Petroleum & Minerals,
   Dhahran 31261, Saudi Arabia

[4]   Department of Chemistry, Indian Institute of Technology,
   Banaras Hindu University, Varanasi 221005, India